# pH-dependent regulation of lysosomal calcium in macrophages

**Kenneth A. Christensen[1,*], Jesse T. Myers[2] and Joel A. Swanson[1,2]**

[1]Department of Microbiology and Immunology and [2]The Program in Cellular and Molecular Biology, University of Michigan Medical School, Ann Arbor, MI 48109-0620, USA

*Author for correspondence (e-mail: kenchris@umich.edu)

*Accepted 22 October 2001*
*Journal of Cell Science 115, 599-607 (2002) © The Company of Biologists Ltd*

## Summary

**Calcium measurements in acidic vacuolar compartments of living cells are few, primarily because calibration of fluorescent probes for calcium requires knowledge of pH and the pH-dependence of the probe calcium-binding affinities. Here we report pH-corrected measurements of free calcium concentrations in lysosomes of mouse macrophages, using both ratiometric and time-resolved fluorescence microscopy of probes for pH and calcium. Average free calcium concentration in macrophage lysosomes was 4-6×10$^{-4}$ M, less than half of the extracellular calcium concentration, but much higher than cytosolic calcium levels. Incubating cells in varying extracellular calcium concentrations did not alter lysosomal pH, and had only a modest effect on lysosomal calcium concentrations, indicating that endocytosis of extracellular fluid provided a small but measurable contribution to lysosomal calcium concentrations. By contrast, increases in lysosomal pH, mediated by either bafilomycin $A_1$ or ammonium chloride, decreased lysosomal calcium concentrations by several orders of magnitude. Re-acidification of the lysosomes allowed rapid recovery of lysosomal calcium concentrations to higher concentrations. pH-dependent reductions of lysosomal calcium concentrations appeared to result from calcium movement out of lysosomes into cytoplasm, since increases in cytosolic calcium levels could be detected upon lysosome alkalinization. These studies indicate that lysosomal calcium concentration is high and is maintained in part by the proton gradient across lysosomal membranes. Moreover, lysosomes could provide an intracellular source for physiological increases in cytosolic calcium levels.**

Key words: Lysosome, Endocytosis, Bafilomycin $A_1$

## Introduction

Despite the importance of calcium in cellular regulation and signal transduction, its concentration in lysosomes remains unknown. Metazoans maintain millimolar concentrations of calcium extracellularly and in ER while holding cytosolic free calcium ($[Ca^{2+}]_{cyt}$) at nanomolar concentrations (Williams, 1999). Measurements of calcium in lysosomes ($[Ca^{2+}]_{lys}$) have been hampered by the effects of low pH on calcium probes. With the absence of such measurements, it has been difficult to examine the roles of lysosomal calcium in cytoplasmic signaling, lysosome physiology, or microbial pathogenesis.

Unlike calcium, pH in vacuolar compartments has been well characterized. Lysosomes maintain a pH of 4.0-5.0, and the intermediate compartments, comprised of pinosomes, phagosomes, early endosomes and late endosomes, are less acidic (Mellman et al., 1986). Macropinosomes, which are formed from cell surface ruffles that close into endocytic vesicles containing extracellular fluid (pH 7.2), acidify within 10 minutes to pH 5.5 (Tsang et al., 2000). Rapid acidification is also characteristic of phagosomes and endosomes (Fuchs et al., 1989; Hackam et al., 1999; McNeil et al., 1983). Experimental alkalinization of vacuolar compartments has indicated requirements for acidic pH in a number of cellular processes, including antigen presentation (Watts, 1997), delivery of toxins and viral capsids across endosomal membranes (Draper and Simon, 1980; Lord et al., 1999; Marsh and Helenius, 1980) and bacterial escape from phagosomes (Beauregard et al., 1997). Hence, it is commonly assumed that pH is the chief controlling variable in vacuolar regulation mechanisms. Other ions found in vacuolar compartments, such as calcium, could be of comparable importance. However, these ions have been more difficult to measure and manipulate in acidic compartments. The elucidation of their relative importance and roles has awaited development of appropriate analytical strategies.

The calcium-binding affinities of the many fluorescent probes for measuring calcium are sensitive to pH, ionic strength and temperature (Grynkiewicz et al., 1985; Lattanzio and Bartschat, 1991; Tsien, 1980). Thus, accurate fluorometric measurement of vacuolar $[Ca^{2+}]$ at constant temperature and ionic strength requires knowledge of compartment pH, as well as the $K_d$ of the fluorescent probe for calcium at that pH, temperature and ionic strength. The reported measurements of calcium in endosomes and phagosomes have identified dramatic decreases in $[Ca^{2+}]$ in those compartments relative to extracellular calcium ($[Ca^{2+}]_{ext}$) (Gerasimenko et al., 1998; Lundqvist et al., 2000). However, these studies probably underestimated calcium concentrations, because experiments designed to measure the effects of pH on probe calcium-binding affinity were carried out using saturating levels of calcium. To measure calcium accurately in acidic environments, both probe calcium-binding affinities and pH must be known precisely.

The present studies characterized calcium dynamics in macrophage vacuolar compartments using four experimental stages. First, the calcium-binding affinities of fluorescent probes were measured over the range of pH found in these compartments. Second, both pH and free calcium were measured in individual organelles using ratiometric fluorescence microscopy and the calibrated fluorescent probes. These measurements were used to obtain pH-corrected values of $[Ca^{2+}]_{lys}$. Third, as a confirmation of the ratiometric measurements, lysosomal calcium concentrations were measured by fluorescence lifetime imaging microscopy. Finally, pharmacological manipulations were applied to examine the relationships between vacuolar calcium, vacuolar pH, and endocytosis. We report that lysosomes contain high concentrations of calcium, and that lysosomal calcium content is influenced by both endocytosis and lysosomal pH. This newfound relationship between pH and vacuolar calcium in macrophages has important implications for organelle trafficking and cellular phenomena presently thought to be regulated by vacuolar pH.

## Materials and Methods

### Reagents

Nigericin and all fluorophores were from Molecular Probes (Eugene, OR), with the exception of FFP-18AM, which was obtained from TEFLabs (Austin, TX). Other reagents were obtained from Sigma Chemical Co. (St Louis, MO), except for the $K^+$ salt of BAPTA (TEFLabs, Austin, TX), ionomycin (Calbiochem, La Jolla, CA), and rM-CSF (R&D Systems, Minneapolis, MN).

### Cell culture

Mouse bone-marrow-derived macrophages were obtained from the femurs of female C57Bl/6 mice (Jackson Laboratories, Bar Harbor, ME) and were cultured in vitro as previously described (Swanson, 1989). Five to eight days after starting the culture, cells were plated onto 25 mm circular coverslips in 6-well dishes at a density of $2\times10^5$ cells/cover slip and incubated overnight in DME, with 10% heat-inactivated FBS and 100 U/ml pen-strep (DME-10F; Gibco BRL, Gaithersburg, MD). Some experiments used macrophages that were activated by overnight incubation in DME-10F with 100 ng/ml LPS (List Biological, Campbell, CA) and 100 U/ml IFN-γ (R&D Systems).

### Determination of fluorescent probe equilibrium dissociation constants

Calcium-binding affinities of fluorescent probes were measured in calibration buffer (CB; 130 mM KCl, 1 mM $MgCl_2$, 15 mM Hepes, 15 mM MES, pH 4-7.2) at 20-22°C. Solutions in which calcium concentrations were ≤40 μM were prepared using EGTA (neutral pH) or BAPTA (lower pH) calcium buffers. Briefly, a 100 mM stock solution of CaEGTA was prepared using the 'pH-metric' method described previously (Tsien and Pozzan, 1989). A 100 mM stock of $K_2$EGTA was also prepared. Similar stock solutions were prepared using BAPTA (100 mM CaBAPTA and 100 mM $K_2$BAPTA). By changing the molar ratio of CaEGTA and $K_2$EGTA, calcium buffers were produced with ionized calcium levels that ranged from 17 nM to 38 μM under neutral pH conditions. Other calcium solutions (≥40 μM ionized calcium) were prepared from a 1 M stock solution of anhydrous $CaCO_3$ that was first boiled to drive off $CO_2$ then pH-adjusted to 7.2 with 5 M HCl.

Calibration of the ratiometric calcium probe fura dextran (furaDx) was performed by measuring the steady state fluorescence excitation spectra of dyes in solutions of known pH and calcium concentration. Excitation wavelengths were varied from 300-420 nm (5 nm band pass) and fluorescence recorded at 510 nm (10 nm band pass) using a spectrofluorometer (PTI, Trenton, NJ). At each pH and calcium concentration, fluorescence spectra were recorded, then analyzed by plotting log $[Ca^{2+}]_{free}$ vs log 340-380 ratio for furaDx and determining the x-intercept. Microsoft Excel Visual Basic programs were used for spectral acquisition and data analysis. Data analysis used methods previously described (Grynkiewicz et al., 1985).

Analogous calibrations were obtained for the fluorescence lifetime probe Oregon Green BAPTA-1 dextran (OGBDx). Fluorescence lifetime decays were recorded on a modified spectrofluorometer (PTI, Trenton, NJ). A 520 nm long pass filter selected the fluorescence emission wavelength illuminating a fast photomultiplier (R6780; Hamamatsu, Japan) connected to time-correlated single photon counting electronics and control software (TimeHarp; Picoquant A/G, Germany). Pulsed excitation was provided from a picosecond mode-locked Ti:Sapphire laser that was pumped by a frequency-doubled Nd:$YVO_4$ solid-state laser (Spectra Physics, Santa Clara, CA). The near infrared output from the Ti:Sapphire laser was pulse-picked to 8 MHz repetition and frequency doubled to 490 nm. The laser was coupled to the spectrofluorometer via a graded-index multi-mode optical fiber. Fluorescence decays were acquired as a function of solution calcium concentration and data was processed using FluoFit software (PicoQuant A/G, Germany) by fitting to a double exponential decay model and determining the fraction of $[Ca^{2+}]_{bound}$ and $[Ca^{2+}]_{free}$ probe. The $K_d$ was obtained by calculating $[Ca^{2+}]_{free}$ where $[Ca^{2+}]_{bound}/[Ca^{2+}]_{free}=1$.

FuraDx and OGBDx remained soluble at the pH values used in these studies. The solubility of BAPTA-based probes is somewhat reduced below pH 6.0, but at low concentrations it remains soluble at pH ≥3 (Tsien, 1980). However, in our studies the $Ca^{2+}$-binding moiety was coupled to dextran, a highly soluble sugar, which increased solubility over a wide pH range. To maintain solubility, all probe solutions were diluted to ≤1 mg/ml, well below the manufacturer's specified solubility limit. To test whether all probe was dissolved under the conditions of the experiments, we examined solutions of dissolved probe by light scattering. Since insoluble probe would increase scattering, we compared the 90° scattering from solutions of furaDx at pH 4-7.2. No significant increase in light scattering was observed, indicating that solubility issues did not complicate our analysis.

### Fluorescent labeling of lysosomes

Macrophage lysosomes were labeled by endocytosis of both pH and calcium probes. Cells on coverslips were washed three times with Ringer's buffer (RB; 155 mM NaCl, 5 mM KCl, 2 mM $CaCl_2$, 1 mM $MgCl_2$, 2 mM $NaH_2PO_4$, 10 mM Hepes and 10 mM glucose, pH 7.2-7.4) and placed in a Leiden chamber (Harvard Apparatus, Cambridge, MA). Macrophages were then pulsed for 15 minutes at 37°C with 0.3-1.0 mg/ml fluorescein dextran (FDx), 0.3-1.0 mg/ml Oregon Green dextran (OGDx), and 1 mg/ml fura dextran (furaDx); all dextrans had an average molecular weight of 10,000. All lysosomal fluorescent probes were dissolved in RB or $Ca^{2+}$-free RB (pH 7.2-7.4) at concentrations ≤1 mg/ml. Loading solutions also contained 10 ng/ml rM-CSF, to stimulate pinocytosis. The cells were washed five times with RB, chased for ≥120 minutes in RB at 37°C, and observed using the ratiometric fluorescence microscope. For experiments in which cells were treated with <2 mM calcium, the cells were pulsed as described above, then chased for ≥120 minutes in calcium-free RB supplemented with calcium from a 400 mM $CaCO_3$ stock solution.

For fluorescence lifetime measurements, macrophage lysosomes were loaded with Oregon Green BAPTA-1 dextran (OGBDx; 1 mg/ml, average molecular weight 10,000) by pulse-labeling for 15 minutes as described above. These cells were washed five times in RB, chased for ≥120 minutes in RB at 37°C and observed using the fluorescence lifetime imaging microscope.

### Measurement of lysosomal pH and $[Ca^{2+}]_{lys}$ using ratiometric fluorescence microscopy

Fluorescence images of labeled cells ($\lambda_{em}$=510 nm) were collected using 340 nm, 380 nm, 440 nm and 485 nm excitation. Images collected at these four excitation wavelengths allowed calculation of both pH and $Ca^{2+}$ levels; 340 nm corresponds to the excitation maximum of calcium-bound furaDx, while 380 nm is the excitation maximum of calcium-free furaDx. The intensity of the FDx and OGDx fluorescence at 440 nm excitation is pH-independent, while fluorescence at 485 nm excitation changes as a function of pH. Consequently, pH was determined from the FDx and OGDx fluorescence (440/485 ratios), and calcium was measured from the furaDx fluorescence (340/380 ratios) using appropriate probe $K_d$ for the measured pH of the organelle.

All images were processed using Metamorph software. Prior to or following each experiment, a background image was collected while blocking the excitation source and leaving all other parts of the light path unchanged. This background image was subtracted from all other images. In addition, fluorescent background signals were determined by histogram analysis of cell-free regions of each image; these were also subtracted from other images.

To obtain an organelle pH ratio, the background-subtracted 485 nm image ($I_{485}$bs) was divided by the background-subtracted 440 nm image ($I_{440}$bs) and multiplied by 1000 to obtain a ratio image ($R_{485/440}$=1000×$I_{485}$bs/$I_{440}$bs). Next, a binary image was generated from the two primary fluorescence images (Binary$_{485}$*$_{440}$= $I_{485}$bs×$I_{440}$bs), adjusting the intensity threshold to include only the labeled organelles. By overlaying that binary image onto the ratio image, measurements of ratios could be restricted to the organelles of interest, and then exported to Excel for further data processing.

Organelle pH was calibrated by equilibrating fluorescently labeled macrophages for at least 10 minutes in CB (pH 3.5-7.2) containing 10 μM of the $H^+$ ionophore nigericin and 10 μM of the $K^+$ ionophore valinomycin. Fluorescence images were acquired at various extracellular pH levels using excitation at 440 nm and 485 nm (Beauregard et al., 1997). These images were processed as described above to obtain a pH standard curve for calibrating the experimental pH ratio values. In organelles loaded with both FDx and OGDx, plots of average intensity ratios ($R_{485nm/440nm}$) vs pH gave a nearly linear response between pH 7.2 and 3.5, as has been shown previously (Downey et al., 1999). These points were fit using a linear least squares algorithm and used to convert intensity ratios to pH values.

To measure calcium ratios, background-subtracted 340 nm and 380 nm images were combined into ratio images ($R_{340/380}$= 1000×$I_{340}$bs/$I_{380}$bs), and the fluorescence ratios of individual organelles were collected and exported to Excel spreadsheets, using binary masks as described above for pH measurements. Calcium probes were calibrated by first incubating labeled macrophages with nigericin and valinomycin in CB (pH 7.2) for 10-15 minutes, then adding ionomycin (final concentration 10 μM**)** and $K_2$EGTA (final concentration 10 mM) and incubating for an additional 3-5 minutes. Fluorescence images were recorded using appropriate excitation wavelengths (340 nm and 380 nm) and the resulting ratio was used to estimate the value in the absence of calcium (i.e. $R_{min}$). This buffer was then replaced with 10 μM ionomycin with excess (10 mM) $Ca^{2+}$ in CB (pH 7.2) and incubated for 3-5 minutes; images were recorded at the appropriate excitation wavelengths to yield the ratio for bound probe (i.e. $R_{max}$). All images were background-subtracted, as described above. Values for $R_{min}$ and $R_{max}$ and Q (the ratio of the fluorescence of the unbound probe at high and low calcium at 380 nm excitation) were used to calculate $[Ca^{2+}]_{lys}$ according to the method described previously (Grynkiewicz et al., 1985). The $K_d$ used for calcium estimation was calculated according to the measured pH of each individual organelle using the constants for BAPTA from Tsien (Tsien, 1980) and the methods for correcting the $K_d$ for temperature, ionic strength and pH of Bers et al. (Bers et al., 1994).

### Measurement of $[Ca^{2+}]_{lys}$ using fluorescence lifetime imaging microscopy

Macrophage lysosomes were loaded with OGBDx by endocytosis as described above. $[Ca^{2+}]_{lys}$ was subsequently obtained with the fluorescence lifetime imaging microscope, using the ratio of two defined delay times after the laser pulse: 1.0 nanosecond ($T_1$) and 3.0 nanoseconds ($T_2$). The ratio of the amplitude of the free ($T_1$) and calcium-bound ($T_2$) probes, obtained during nanosecond measurement windows was used to obtain the overall free calcium concentration. These results were calibrated using a similar approach to the ratiometric measurements described above except that $R_{min}$ and $R_{max}$ were determined from the ratio of $T_1/T_2$, and $8.74\times10^{-4}$ M (pH 4.0) was used for the probe $K_d$.

### Measurement of $[Ca^{2+}]_{cyt}$

FFP-18AM, a fura-2-like probe that labels cell membranes, was dissolved in DMSO and loaded into macrophages as an acetoxymethyl ester. Cells were incubated for 30 minutes at 37° in RB containing 1 μM FFP-18 AM and 1% Pluronic F-127 (Calbiochem, La Jolla, CA), washed with RB prior to measurement. Fluorescence images were acquired using 340 and 380 nm excitation ($\lambda_{em}$=510 nm). After appropriate background subtraction, as described for measurement of organelle pH and $[Ca^{2+}]_{lys}$ using ratiometric fluorescence microscopy, a binary image was generated by adjusting the intensity threshold to include only the labeled cells. By overlaying the binary image onto the two images, ratio measurements of labeled cells were collected for export to Excel and further data processing. Ratios were calibrated using the $Ca^{2+}$ ionophore ionomycin, as described above.

### Manipulation of pH, calcium and magnesium

Lysosomal pH was increased using bafilomycin $A_1$ (final concentration 500 nM from a 100 μM stock in DMSO) or ammonium chloride (final concentration 10 mM), added to cells in RB.

All experiments were performed in the presence of millimolar $Mg^{2+}$. Since the affinity of BAPTA for $Mg^{2+}$ is several orders of magnitude lower than its affinity for calcium, interferences from $Mg^{2+}$ were not expected. However, as a control experiment, macrophage lysosomes were loaded with the pH and calcium probes using our standard protocols, then chased for ≥120 minutes in $Mg^{2+}$-free RB prior to making the measurements. Additionally, pH and calcium calibrations were performed in $Mg^{2+}$-free CB.

### Microscopy

#### Ratiometric imaging

Ratiometric images were acquired using an inverted research microscope (TE300; Nikon, Japan) equipped with phase-contrast transmitted light and mercury arc lamp excitation with epi-fluorescence optics. Several dichroic mirror sets (Omega Optical, Brattleboro, VT) were used; a double excitation set for both fura and fluorescein dyes (XF79: 340HT15, 380HT15, 440DF20, 485DF15 excitation filters in wheel; 505DRLPXR dichroic mirror and 535DF35 emission filter in cube) was used for the majority of experiments, while a single generic blue dichroic (XF12: 340HT15 and 380HT15 excitation filters in wheel; 420DCLP dichroic mirror and 435ALP emission filter in cube) was used where necessary to increase microscope sensitivity for the fura-based calcium probes. An excitation filter wheel (Lambda 10-2, Sutter Instruments, Novato, CA), containing band pass filters, was used to select the excitation wavelength. Both the transmitted light path and the fluorescence excitation path contained shutters (Uniblitz, Rochester, NY) to control illumination of the cells. A temperature-controlled imaging chamber (Harvard Apparatus, Cambridge, MA) maintained sample temperature at 37°C. A cooled scientific CCD camera (Quantix;

Photometrics, Tucson, AZ) recorded fluorescence and transmitted light images. For some experiments a lens-coupled GEN IV intensifier (VSH-1845; Videoscope Intl., Dulles, VA) was inserted in front of the CCD camera. Metamorph software (Universal Imaging, West Chester, PA) controlled the camera, shutters, and filter wheels during all experiments.

### Fluorescence lifetime imaging

The fluorescence lifetime imaging microscope was an inverted research grade microscope (TE300; Nikon, Japan) equipped with both phase-contrast and epi-fluorescence optics and shutters (Uniblitz, Rochester, NY). Fluorescence excitation was provided via a graded index multi-mode fiber optic, coupled to a mode-locked Ti:Sapphire laser (Tsunami, 1 picosecond pulses, 81 MHz, 835-1005 nm; Spectra Physics, Mountain View, CA), which was pulse picked to 8 MHz and frequency doubled (415-500 nm), and pumped by a solid-state frequency-doubled Nd:$YVO_4$ laser (532 nm, Millennia V; Spectra Physics, Mountain View, CA). The fiber was mechanically agitated to scramble the coherence of the laser. A dichroic mirror set (XF115: 475AF40 excitation filter, 505DRLP dichroic mirror, and 510ALP emission filter in the cube, Omega Optical, Brattleboro, VT) reflected the excitation light onto the sample and selected for the green fluorescence prior to the picosecond gated intensified CCD camera (PicoStar HR; LaVision A/G, Germany). A DEL-150 computer board (Becker & Hickl A/G, Germany) produced electronic time delays relative to the laser pulse. DaVis software (LaVision A/G, Germany) controlled the camera, laser shutter, and delay board during image acquisition. For these experiments, images were collected in 1000 picosecond windows, with delay times of 1.0 and 3.0 nanoseconds after the pulse. Images of fluorescence at the two delay times were then analyzed ratiometrically to infer changes in fluorescence lifetimes of the fluorophores.

## Results

### Determination of pH-dependence of calcium sensor affinity

Measurements of intracellular [$Ca^{2+}$] are typically obtained using fluorescent probes covalently attached to calcium chelators. Such probes include furaDx (ratiometric) and OGBDx (fluorescence lifetime). FuraDx changes its excitation spectrum upon binding calcium, similar to the widely used probe fura-2. Free calcium concentrations were determined by acquiring images at the fluorescence excitation maxima for both calcium-bound and calcium-free forms of these probes (340 nm and 380 nm, respectively), then measuring the ratio of the fluorescence intensities from the two images. Unlike furaDx, the fluorescence lifetime of OGBDx varies with free calcium concentration. As a result, this probe was used to measure lysosomal calcium concentrations using wide field fluorescence lifetime imaging, rather than ratiometric imaging. Like ratiometric imaging, fluorescence lifetime imaging allows for quantitative determination of solution calcium despite variable path lengths, probe concentrations and photobleaching.

Because chelator affinity for calcium is altered by pH, fluorescent calcium probes are typically used within a limited pH range. The calcium probes used in this study are structural variants of the calcium chelator BAPTA, whose calcium affinity remains relatively constant between pH 6.0 and pH 7.5 (Tsien and Pozzan, 1989), but changes by several orders of magnitude between pH 6.0 and 4.0. Calcium levels are typically calculated from the probe's fluorescent response assuming that the reported $K_d$, measured at neutral pH, applies over the pH range of the experiments. Such assumptions are useful above pH 6.0, but are invalid at lower pH ranges where the probe $K_d$ is more sensitive to solution pH. Hence, to use BAPTA-based probes at low pH, the probe's $K_d$ for calcium at that pH must be accurately known and applied to the calculation of [$Ca^{2+}$]. To determine the relationship between probe $K_d$ and pH, the calcium-binding affinities of the calcium probes were measured between pH 4.0 and 7.0. The affinities of furaDx and OGBDx for calcium were similar to those previously described for BAPTA (Fig. 1) (Tsien, 1980; Bers et al., 1994). This result was not surprising, considering the structural similarities between the calcium-binding moieties of furaDx, OGBDx and BAPTA. Further, this result indicated that published relationships between solution pH and BAPTA affinity for calcium (Tsien, 1980; Bers et al., 1994) could be used to calibrate the measurements with furaDx and OGBDx.

This relationship between probe affinity and solution pH allowed us to measure [$Ca^{2+}$] over a large pH range (4.0-7.2). As for any equilibrium probe, the highest probe sensitivity is obtained when measured [$Ca^{2+}$] is within a log unit of the $K_d$. Thus, optimal measurement is a function of both probe $K_d$, which varies with pH, and solution [$Ca^{2+}$]. At pH 4.0, furaDx and OGBDx reliably measured calcium between $10^{-2}$ and $10^{-4}$ M; at higher pH, probe $K_d$ was lower, and the range of measurable [$Ca^{2+}$] was also lower (e.g. $10^{-4}$ to $10^{-6}$ M at pH 5.0). Although nearly all measurements were within this measurement window, we discarded data in which the [$Ca^{2+}$] fell outside one log unit of the probe $K_d$.

### Measurement of $[Ca^{2+}]_{lys}$

To measure calcium in macrophage lysosomes, a fluorescent probe cocktail containing FDx, OGDx and furaDx was loaded into lysosomes by endocytosis. Upon visualization in the microscope, the dyes were compartmentalized in tubular and

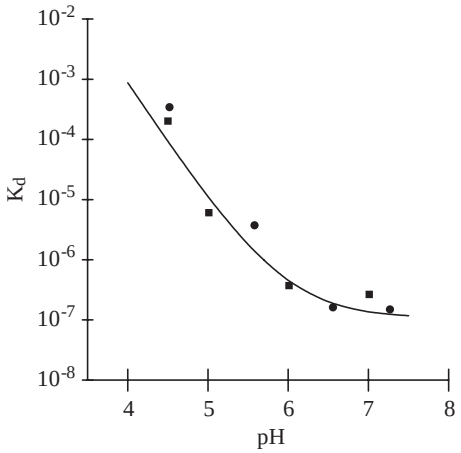


**Fig. 1.** Plot of measured calcium $K_d$ as a function of pH for the fluorescent calcium probes furaDx (■) and OGBDx (●). The solid line represents the predicted $K_d$ of BAPTA using the constants measured by Tsien (Tsien, 1980) and the methods of Bers et. al. (Bers et al., 1994) to correct for temperature, ionic strength and pH. All measurements were performed at 22°C with constant ionic strength (0.130 M) and variable pH (4-7.2) in Hepes/MES pH buffers containing 1 mM $Mg^{2+}$.

vesicular structures typical of lysosomes and late endosomes (Swanson et al., 1987; Swanson, 1999), indicating that the probes were effectively trafficked to lysosomal compartments within the cell.

The spectral responses of FDx and OGDx were used to determine pH of individual lysosomes, which was then used to calibrate the spectral response of furaDx in those same organelles. Lysosomal pH was 4.0±0.1 and measured lysosomal furaDx ratios nearly all fell between $R_{min}$ and $R_{max}$. Using the calculated relationship between pH and probe affinity (Fig. 1), $[Ca^{2+}]_{lys}$ was determined to be $6.0\pm0.9\times10^{-4}$ M ($n$=24 cells; Fig. 2).

To corroborate the ratiometric fluorescence imaging results, $[Ca^{2+}]_{lys}$ was also measured by fluorescence lifetime imaging, using the fluorescence lifetime probe OGBDx. Lifetime measurements did not allow simultaneous measurement of both pH and calcium in individual organelles, so we calibrated OGBDx using its $K_d$ at pH 4.0, as determined by the ratiometric measurements. Fluorescence lifetime microscopic measurement of OGBDx reported a $[Ca^{2+}]_{lys}$ of $4.0\pm0.7\times10^{-4}$ M ($n$=18 cells; Fig. 2), similar to that obtained using ratiometric methods. Thus, $[Ca^{2+}]_{lys}$ was found by two different methods to be lower than extracellular calcium ($[Ca^{2+}]_{ext}$=2 mM) and substantially higher than the cytosolic calcium concentrations ($[Ca^{2+}]_{cyt}$=50-150 nM).

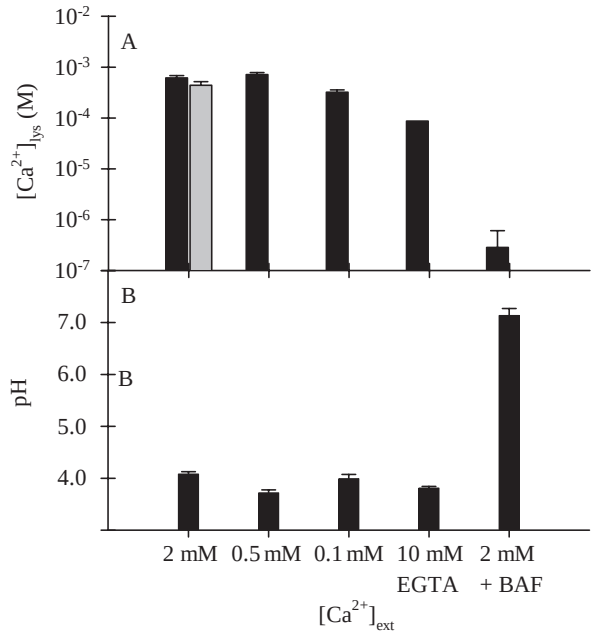


**Fig. 2.** $[Ca^{2+}]_{lys}$ and lysosomal pH: resting levels and effects of variable extracellular calcium and bafilomycin $A_1$. (A) $[Ca^{2+}]_{lys}$. Black bars represent ratiometric measurements using a probe cocktail consisting of furaDx, FDx, and OGDx. The gray bar represents calcium measurements using fluorescence lifetime imaging with the calcium indicator OGBDx. The fluorescence ratio of furaDx was ≤$R_{min}$ for cells incubated in 10 mM EGTA, therefore $[Ca^{2+}]_{lys}$ was below the detection limit for furaDx at pH 4 (the bar represents the detection limit of furaDx at pH 4). Error bars represent s.e.m. ($n$≥10 cells). (B) Lysosomal pH. Error bars represent s.e.m. ($n$≥10 cells).

### Measurements of $[Ca^{2+}]_{lys}$ in the absence of magnesium

As all experiments were performed in the presence of millimolar $Mg^{2+}$, it was possible that probe response reflected $[Mg^{2+}]$ instead of, or in addition to, $[Ca^{2+}]$. Since the affinity of BAPTA for $Mg^{2+}$ is several orders of magnitude lower than its affinity for calcium, interferences from $Mg^{2+}$ were not expected. However, in light of previous biological roles proposed for $Mg^{2+}$, interpretation of our $Ca^{2+}$ measurements required that we examine the effects of $[Mg^{2+}]$ on our measurements. $[Ca^{2+}]_{lys}$ was measured in RB without added $Mg^{2+}$, calibration of the probe's fluorescence response was performed in the absence of $Mg^{2+}$ ($Mg^{2+}$-free CB), and ratiometric fluorescence measurements in $Mg^{2+}$-free and $Mg^{2+}$-containing buffers were compared. As predicted from in vitro measurements, there were no significant differences between the ratiometric fluorescence measurements of pH and $[Ca^{2+}]_{lys}$ in the presence or absence of $Mg^{2+}$ (data not shown), indicating that $Mg^{2+}$ has no measurable effect on the fluorescence response of the calcium probes.

### Changes in $[Ca^{2+}]_{ext}$ and $[Ca^{2+}]_{cyt}$ affect $[Ca^{2+}]_{lys}$

Lysosomal calcium levels may result from calcium influx into the lysosomes via endocytosis. To ascertain the role of endocytosis in determining measured lysosomal calcium levels, we labeled the lysosomes with furaDx and the pH probe cocktail, then incubated cells in a range of extracellular calcium concentrations. $[Ca^{2+}]_{lys}$ was similar in cells incubated in RB containing 2 mM calcium or 500 μM calcium, but was slightly reduced in cells incubated with RB containing 100 μM calcium (Fig. 2). These results suggest that influx of calcium via endocytosis contributes to the high $[Ca^{2+}]_{lys}$. $[Ca^{2+}]_{lys}$ was also measured in cells that had been incubated in the absence of $Ca^{2+}$. In cells chased in 10 mM EGTA, $[Ca^{2+}]_{lys}$ dropped to ≤$10^{-5}$ M. $[Ca^{2+}]_{lys}$ lower than $10^{-5}$ M could not be detected with furaDx because of the low pH. Since the $K_d$ of CaEGTA at pH 4 is nearly 1 M, the EGTA inside the lysosomes was probably not buffering $[Ca^{2+}]_{lys}$ to low levels. Instead, extracellular EGTA should have had two different effects that would lower $[Ca^{2+}]_{lys}$. First, by reducing $[Ca^{2+}]_{ext}$, it reduced the amount of calcium entering lysosomes by endocytosis. Second, because EGTA can reduce $[Ca^{2+}]_{cyt}$ to low levels (Larsen et al., 2000), it may have depleted lysosomes of calcium through its effect on $[Ca^{2+}]_{cyt}$ (see below). Thus, $[Ca^{2+}]_{lys}$ may be affected by both $[Ca^{2+}]_{ext}$ and $[Ca^{2+}]_{cyt}$. In cells that were chased in different calcium concentrations or in EGTA, lysosomal pH remained constant (Fig. 2), indicating that the altered lysosomal $Ca^{2+}$ levels do not affect lysosomal pH.

### Increasing lysosomal pH reduces $[Ca^{2+}]_{lys}$

Experimental manipulation of pH levels have allowed identification of important roles for vacuolar acidification in physiology and pathogenesis. It is possible that lysosomal pH could also affect lysosomal $Ca^{2+}$ levels. To determine the relationship between lysosomal pH and $[Ca^{2+}]_{lys}$, $[Ca^{2+}]_{lys}$ was measured after manipulation of lysosomal pH. Macrophages were treated with bafilomycin $A_1$, an inhibitor of the $H^+$-ATPase that increases pH of acidic compartments. After 45 minutes in bafilomycin $A_1$, lysosomal pH increased from 4 to

7 and $[Ca^{2+}]_{lys}$ decreased from 0.6 mM to 285 nM (Fig. 2). We next examined the time-course of this effect (Fig. 3). Cells incubated for 1-3 hours in RB without bafilomycin $A_1$ maintained constant low pH and high $[Ca^{2+}]_{lys}$ (data not shown). However, after addition of bafilomycin $A_1$, pH increased from 4 to 7 over 45 minutes, and $[Ca^{2+}]_{lys}$ decreased correspondingly. These results demonstrate a profound relationship between lysosomal pH and $[Ca^{2+}]_{lys}$.

It was possible that this dramatic result reflected a process unique to bafilomycin $A_1$. Hence, the pH-dependence of $[Ca^{2+}]_{lys}$ was also examined using the weak base ammonia, which rapidly increases the pH of acidic compartments (Poole and Ohkuma, 1981). Within 60 seconds of adding 10 mM ammonium chloride, pH increased and $[Ca^{2+}]_{lys}$ decreased in magnitude similar to that observed using bafilomycin $A_1$ (Fig. 4). Returning cells to RB without ammonium chloride produced a rapid reacidification and recovery of high $[Ca^{2+}]_{lys}$. Together, these studies indicated that although $[Ca^{2+}]_{lys}$ did not affect lysosomal pH (Fig. 2), lysosomal pH had a profound effect on $[Ca^{2+}]_{lys}$.

### Elevation of lysosomal pH released calcium into the cytoplasm

Two mechanisms could account for the pH-dependence of $[Ca^{2+}]_{lys}$. First, pH-dependent calcium-binding molecules present in the organelle could selectively bind calcium at increased pH, leading to lysosomal sequestration of calcium and reduced $[Ca^{2+}]_{lys}$. Second, pH-dependent calcium channels or transporters could release calcium from the lysosome into the cytosol at increased pH. These possibilities can be distinguished by measuring $[Ca^{2+}]_{cyt}$ as lysosomal pH is increased, since calcium released from lysosomes during alkalinization should increase $[Ca^{2+}]_{cyt}$. $[Ca^{2+}]_{cyt}$ was measured in macrophages labeled with FFP-18 (Fig. 5A). When lysosomal pH was increased in non-activated macrophages, small increases in cytosolic calcium levels could be observed (data not shown). Significantly larger effects of lysosomal pH on cytosolic calcium were observed in activated macrophages (Fig. 5A), where lower resting cytosolic calcium and larger lysosomal compartments presumably produced greater relative effects on total cytosolic calcium (Cohn, 1978; Lowry et al., 1999). Complementary time-lapse measurements of the rapid drop in $[Ca^{2+}]_{lys}$ associated with elevation of lysosomal pH are shown in Fig. 5B (Fig. 5C shows control). Additionally, similar measurable increases in cytosolic calcium were observed in non-activated macrophages when thapsigargin was used to inhibit calcium uptake by the ER (data not shown). Although these experiments cannot rule out calcium efflux into the cytosol from other calcium storage organelles, the effects of ammonium chloride would be greatest upon the most acidic organelles (i.e. lysosomes). Therefore, these results indicated that calcium was being released from lysosomes into cytosol upon alkalinization. The reduced $[Ca^{2+}]_{lys}$ observed at increased pH may reflect the presence of pH-dependent calcium channels or transporters in the lysosomal membrane.

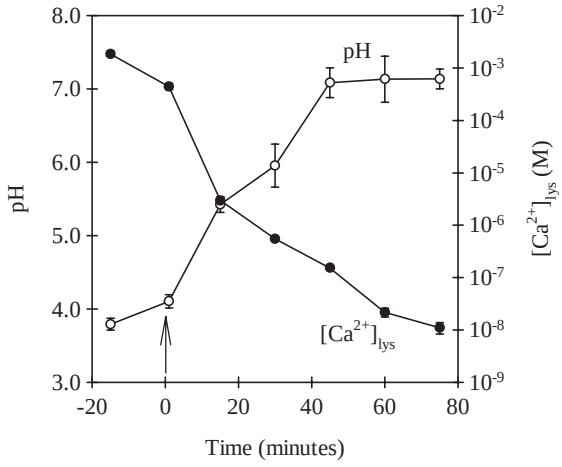


**Fig. 3.** A time course showing ratiometric measurements of lysosomal pH (○) and $[Ca^{2+}]_{lys}$ (●) following the addition of buffer containing 500 nM bafilomycin $A_1$ (BAF). Lysosomes were labeled with a probe cocktail containing furaDx, FDx, and OGDx. Arrow indicates time of BAF addition. Error bars represent the s.e.m. (n≥9 cells).

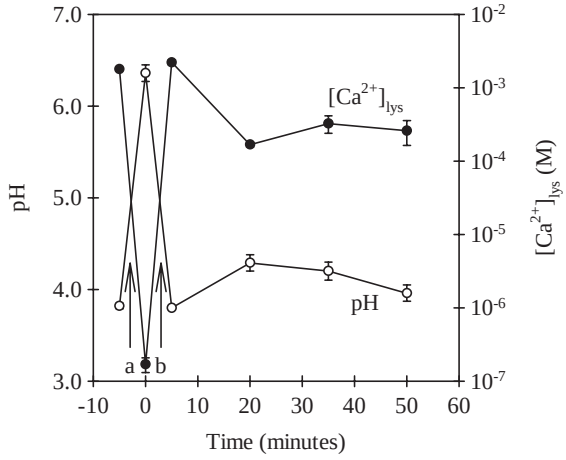


**Fig. 4.** A time course showing ratiometric measurements of lysosomal pH (○) and $[Ca^{2+}]_{lys}$ (●) following the addition of buffer containing 10 mM $NH_4Cl$. Lysosomes were labeled with a probe cocktail containing furaDx, FDx and OGDx. Arrow 'a' indicates time of addition of $NH_4Cl$. Arrow 'b' indicates time of addition of $NH_4Cl$-free buffer (RB) causing rapid reacidification and restoration of high $[Ca^{2+}]_{lys}$. Error bars represent the s.e.m. ($n$≥9 cells).

## Discussion

### Regulation of $[Ca^{2+}]_{lys}$

Two different imaging methods were used to measure $[Ca^{2+}]$ in macrophage lysosomes. These imaging methods overcome technical limitations previously associated with measurements of $[Ca^{2+}]$ at low pH (Gerasimenko et al., 1998; Lundqvist et al., 2000). The present work combined calibration of the pH-dependence of probe affinities for calcium with measurements of both pH and calcium inside individual organelles. These techniques were facilitated by the selection of probes that reliably reported $[Ca^{2+}]$ within a relevant range of pH (i.e. their ratios were between $R_{max}$ and $R_{min}$ and within an order of magnitude of the $K_d$). These pH-corrected measurements showed that macrophage $[Ca^{2+}]_{lys}$ was 400-600 μM, which is

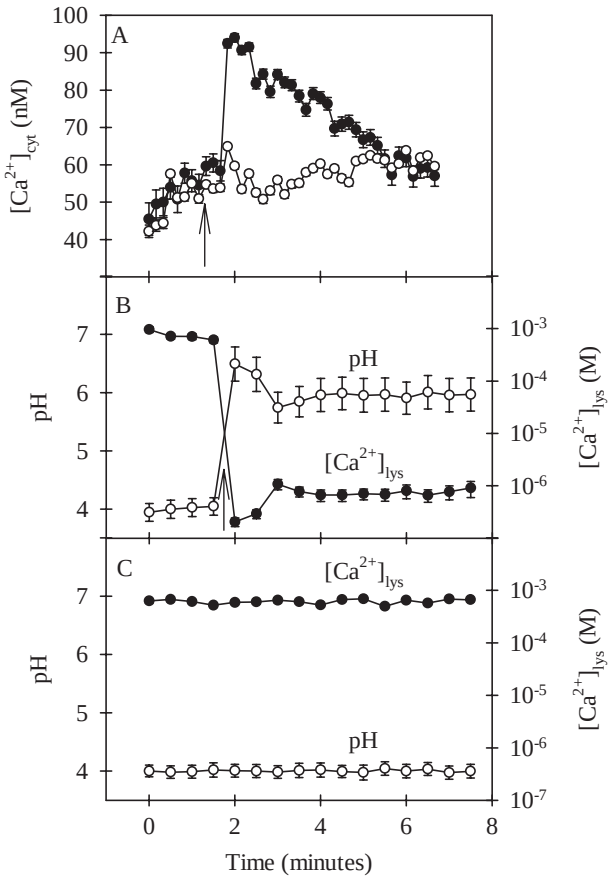


**Fig. 5.** Data from a time-course experiment showing the effects of $NH_4Cl$ on macrophage $[Ca^{2+}]_{cyt}$ and $[Ca^{2+}]_{lys}$. (A) $[Ca^{2+}]_{cyt}$ in activated macrophages (●) following addition of $NH_4Cl$ and control cells (○; activated macrophages without addition of $NH_4Cl$). (B) $[Ca^{2+}]_{lys}$ (●) and lysosomal pH (○) in activated macrophages following addition of $NH_4Cl$. (C) $[Ca^{2+}]_{lys}$ (●) and lysosomal pH (○) in control cells (no $NH_4Cl$ added). To measure $[Ca^{2+}]_{cyt}$, cells were loaded with FFP-18AM. To measure $[Ca^{2+}]_{lys}$, cells were loaded with a probe cocktail consisting of furaDx, FDx, and OGDx. Arrows show times of addition of ammonium chloride. Error bars represent s.e.m. ($n$=30 cells for $[Ca^{2+}]_{cyt}$ measurements and $n \geq 15$ cells for $[Ca^{2+}]_{lys}$ measurements).

less than extracellular calcium concentrations and much higher than $[Ca^{2+}]_{cyt}$. To our knowledge, this is the first report of direct quantitative measurements of $[Ca^{2+}]_{lys}$ in living cells. Our findings are consistent with earlier indirect measurements of $[Ca^{2+}]_{lys}$ (Fujimoto, 1992; Haller et al., 1996).

### The contribution of endocytosis to $[Ca^{2+}]_{lys}$

Vacuolar accumulation of fluid-phase probes by pinocytosis is directly proportional to extracellular concentrations of those probes (Swanson and Silverstein, 1988; Swanson, 1999). If calcium were to behave analogously, its concentration in lysosomes would be proportional to $[Ca^{2+}]_{ext}$. Instead, lowering $[Ca^{2+}]_{ext}$ from 2 mM to 500 μM did not appreciably alter $[Ca^{2+}]_{lys}$, indicating that at or near physiological $[Ca^{2+}]_{ext}$, $[Ca^{2+}]_{lys}$ is regulated independent of endocytosis. However, incubation of cells in 100 μM $[Ca^{2+}]_{ext}$ or in EGTA-containing buffers decreased $[Ca^{2+}]_{lys}$. These observations could be explained by a mechanism in which endocytosis provides a source of calcium for the vacuolar compartment, but other factors prevent $[Ca^{2+}]_{lys}$ from exceeding 600 μM.

### The relationship between lysosomal pH and $[Ca^{2+}]_{lys}$

Alterations of $[Ca^{2+}]_{ext}$ or $[Ca^{2+}]_{lys}$ did not alter lysosomal pH. A previous study of the pH-dependence of $[Ca^{2+}]$ in endocytic compartments, carried out on fibroblast endosomes, showed that increases in extracellular calcium led to reduced acidification (Gerasimenko et al., 1998). The differing results of the two studies suggests that the pH-dependence of $[Ca^{2+}]_{lys}$ may not apply to all endocytic organelles.

Although changing $[Ca^{2+}]_{lys}$ did not measurably affect lysosomal pH, increases in lysosomal pH dramatically lowered $[Ca^{2+}]_{lys}$. Slow alkalinization with bafilomycin $A_1$ produced an equally slow lowering of $[Ca^{2+}]_{lys}$. Rapid alkalinization with ammonium chloride produced a rapid decrease in $[Ca^{2+}]_{lys}$ by several orders of magnitude. Because increases in $[Ca^{2+}]_{cyt}$ could be detected when lysosomal pH was increased with ammonium chloride, we infer that vacuolar calcium was moving into cytoplasm, possibly via pH-dependent calcium channels or pumps.

High $[Ca^{2+}]_{lys}$ was rapidly restored by removal of ammonium chloride, indicating that calcium can be delivered into lysosomes from cytoplasm. Accordingly, the sensitivity of $[Ca^{2+}]_{lys}$ to pH may reflect an equilibrium relationship between pH and calcium across the lysosomal membrane. We propose a mechanism similar to that described for calcium accumulation in yeast vacuoles (Dunn et al., 1994; Ohsumi and Anraku, 1983). First, the proton ATPase in the lysosomal membrane maintains an acidic lumenal pH and a gradient of protons across that membrane. Second, the proton gradient drives the accumulation of calcium via a calcium/proton exchange protein in the lysosomal membrane. Conditions that elevate lysosomal pH reduce the proton gradient and consequently reduce the calcium concentration gradient that can be maintained across that membrane.

### Implications for cell biology and pathogenesis

The most striking finding of the present studies is that experimental treatments that increase the pH of vacuolar compartments in macrophages lower vacuolar calcium levels proportionally. This implies that cellular processes previously attributed to vacuolar acidification may be equally attributable to vacuolar decalcification. These processes could include receptor-ligand dissociation in endosomes, penetration of cellular membranes by bacterial toxins and viral capsids, and the processing and loading of antigen onto MHC class II molecules (Mellman et al., 1986). We have observed reductions in $[Ca^{2+}]_{pino}$ by two orders of magnitude as pH decreases from 7.2 to 6.2 in newly formed pinosomes, followed by significant increases in $[Ca^{2+}]_{pino}$ as the pinosome matures (K.A.C., unpublished), implying that low calcium concentration is a distinct physiological feature of early endosomes. In light of these observations and those described in this study, it may be appropriate to re-examine any processes in which a primary role for pH has not been supported by independent experimental approaches.

This relationship between vacuolar pH and vacuolar calcium could also affect membrane fusion between late endosomes, lysosomes and other organelles. Various studies have demonstrated that raising lysosomal pH increases lysosomal secretion (Tapper and Sundler, 1990), that increasing $[Ca^{2+}]_{cyt}$ leads to lysosomal secretion (Andrews, 1995), and that endocytosed calcium may provide a source of calcium that facilitates vesicle fusion (Peters and Mayer, 1998). Perhaps transient or experimentally induced alkalinization of lysosomes releases calcium that allows membrane fusion with plasma membrane or with other organelles.

Although plasma membrane and ER are the principal regulated sources of cytosolic calcium, the vacuolar compartment could serve as an additional source of $[Ca^{2+}]_{cyt}$. The magnitude of the changes in $[Ca^{2+}]_{cyt}$ observed here in response to alkalinization were small relative to total cytosolic calcium, but it may be that, under some circumstances, transient alkalinization of late endosomes or lysosomes releases sufficient calcium to produce an intracellular signal.

A number of bacterial and fungal pathogens survive within macrophage vacuolar compartments, and their mechanisms for survival may require manipulation or monitoring of vacuolar $[Ca^{2+}]$. For example, survival of *Histoplasma capsulatum* inside macrophage vacuoles requires that organism to secrete a calcium-binding protein (Kugler et al., 2000; Sebghati et al., 2000). This protein could be required to maintain $[Ca^{2+}]$ sufficiently high to allow growth in the relatively alkaline vacuole (Eissenberg et al., 1988). For *Salmonella typhimurium*, regulation of gene expression in phagosomes has been linked with both pH and divalent cations (Alpuche-Arande et al., 1992; Vescovi et al., 1996). A full explanation of this regulatory system will require the development and application of methods for distinguishing the contributions of vacuolar pH and calcium.

The authors wish to thank P. Christine Ackroyd for her help in writing and editing this manuscript. This work was supported by NIH grant AI 35950 to J.A.S.

## References

**Alpuche-Arande, C. M., Swanson, J. A., Loomis, W. P. and Miller, S. I.** (1992). *Salmonella typhimurium* activates virulence gene transcription within acidified phagosomes. *Proc. Natl. Acad. Sci. USA* **89**, 10079-10083.

**Andrews, N. W.** (1995). Lysosome recruitment during host cell invasion by *Trypanosoma cruzi*. *Trends Cell Biol.* **5**, 133-137.

**Beauregard, K. E., Lee, K.-D., Collier, R. J. and Swanson, J. A.** (1997). pH-dependent perforation of macrophage phagosomes by listeriolysin O from *Listeria monocytogenes*. *J. Exp. Med.* **186**, 1159-1163.

**Bers, D. M., Patton, C. W. and Nuccitelli, R.** (1994). A Practical Guide to the Preparation of $Ca^{2+}$ Buffers. In *Methods in Cell Biology*, Vol. 40 (ed. R. Nuccitelli), pp. 3-29. New York: Academic Press Inc.

**Cohn, Z. A.** (1978). The activation of mononuclear phagocytes: Fact, fancy, and future. *J. Immunol.* **121**, 813-816.

**Downey, G. P., Botelho, R. J., Butler, J. R., Moltyaner, Y., Chien, P., Schreiber, A. D. and Grinstein, S.** (1999). Phagosomal maturation, acidification, and inhibition of bacterial growth in nonphagocytic cells transfected with FcγRIIA receptors. *J. Biol. Chem.* **274**, 28436-28444.

**Draper, R. K. and Simon, M. I.** (1980). The entry of diphtheria toxin into the mammalian cell cytoplasm: evidence for lysosomal involvement. *J. Cell Biol.* **87**, 849-854.

**Dunn, T., Gable, K. and Beeler, T.** (1994). Regulation of cellular $Ca^{2+}$ by yeast vacuoles. *J Biol. Chem.* **269**, 7273-7278.

**Eissenberg, L. G., Schlessinger, P. H. and Goldman, W. E.** (1988). Phagosome-lysosome fusion in P388D1 macrophages infected with *Histoplasma capsulatum*. *J. Leukocyte Biol.* **43**, 483-491.

**Fuchs, R., Schmid, S. and Mellman, I.** (1989). A possible role for $Na^+$, $K^+$-ATPase in regulating ATP-dependent endosome acidification. *Proc. Natl. Acad. Sci. USA* **86**, 539-543.

**Fujimoto, T.** (1992). Calcium pump of the plasma membrane is localized in caveolae. *J. Cell Biol.* **120**, 1147-1157.

**Gerasimenko, J. V., Tepikin, A. V., Petersen, O. H. and Gerasimenko, O. V.** (1998). Calcium uptake via endocytosis with rapid release from acidifying endosomes. *Curr. Biol.* **8**, 1335-1338.

**Grynkiewicz, G., Poenie, M. and Tsien, R. Y.** (1985). A new generation of $Ca^{2+}$ indicators with greatly improved fluorescence properties. *J. Biol. Chem.* **260**, 3440-3450.

**Hackam, D. J., Rotstein, O. D. and Grinstein, S.** (1999). Phagosomal Acidification: Mechanisms and functional significance. In *Phagocytosis: The Host*, Vol. 5 (ed. S. Gordon), pp. 299-319. Stamford: JAI Press.

**Haller, T., Dietl, P., Deetjen, P. and Volkl, H.** (1996). The lysosomal compartment as intracellular calcium store in MDCK cells: a possible involvement in InsP3-mediated $Ca^{2+}$ release. *Cell Calcium* **19**, 157-165.

**Kugler, S., Sebghati, T. S., Eissenberg, L. G. and Goldman, W. E.** (2000). Phenotypic variation and intracellular parasitism by *Histoplasma capsulatum*. *Proc. Natl. Acad. Sci. USA* **97**, 8794-8798.

**Larsen, E. C., DiGennaro, J. A., Saito, N., Mehta, S., Loegering, D. J., Mazurkiewicz, J. E. and Lennartz, M. R.** (2000). Differential requirement for classic and novel PKC isoforms in respiratory burst and phagocytosis in RAW 264.7 cells. *J. Immunol.* **165**, 2809-2817.

**Lattanzio, F. A. and Bartschat, D. K.** (1991). The effect of pH on rate constants, ion selectivity and thermodynamic properties of fluorescent calcium and magnesium indicators. *Biochem. Biophys. Res. Commun.* **177**, 184.

**Lord, J. M., Smith, D. C. and Roberts, L. M.** (1999). Toxin entry: how bacterial proteins get into mammalian cells. *Cell. Microbiol.* **1**, 85-91.

**Lowry, M. A., Goldberg, J. I. and Belosevic, M.** (1999). Treatment of the macrophage-like P388D.1 cells with bacterial lipopolysaccharide and interferon-gamma causes long-term alterations in calcium metabolism. *Dev. Comp. Immunol.* **23**, 253-261.

**Lundqvist, H., Gustafsson, M. and Dahlgren, C.** (2000). Dynamic $Ca^{2+}$ changes in neutrophil phagosomes. A source for intracellular $Ca^{2+}$ during phagolysosome formation. *Cell Calcium* **27**, 353-362.

**Marsh, M. and Helenius, A.** (1980). Adsorptive endocytosis of Semliki Forest Virus. *J. Mol. Biol.* **142**, 439-454.

**McNeil, P. L., Tanasugarn, L., Meigs, J. B. and Taylor, D. L.** (1983). Acidification of phagosomes is initiated before lysosomal enzyme activity is detected. *J. Cell Biol.* **97**, 692-702.

**Mellman, I., Fuchs, R. and Helenius, A.** (1986). Acidification of the endocytic and exocytic pathways. *Annu. Rev. Biochem.* **55**, 663-700.

**Ohsumi, Y. and Anraku, Y.** (1983). Calcium transport driven by a proton motive force in vacuolar membrane vesicles of *Saccharomyces cerevisiae*. *J. Biol. Chem.* **258**, 5614-5617.

**Peters, C. and Mayer, A.** (1998). $Ca^{2+}$/calmodulin signals the completion of docking and triggers a late step of vacuole fusion. *Nature* **396**, 575-580.

**Poole, B. and Ohkuma, S.** (1981). Effect of weak bases on the intralysosomal pH in mouse peritoneal macrophages. *J. Cell Biol.* **90**, 665-669.

**Sebghati, T. S., Engle, J. T. and Goldman, W. E.** (2000). Intracellular parasitism by *Histoplasma capsulatum*: Fungal virulence and calcium dependence. *Science* **290**, 1368-1372.

**Swanson, J. A.** (1989). Phorbol esters stimulate macropinocytosis and solute flow through macrophages. *J. Cell Sci.* **94**, 135-142.

**Swanson, J. A.** (1999). Pathways through the macrophage vacuolar compartment. In *Phagocytosis: The Host*, Vol. 5 (ed. S. Gordon), pp. 267-284. Stamford: JAI Press.

**Swanson, J. and Silverstein, S. C.** (1988). Pinocytic flow through macrophages. In *Processing and Presentation of Antigens* (ed. B. Pernis, S. C. Silverstein and H. Vogel), pp. 15-27. New York: Academic Press.

**Swanson, J., Bushnell, A. and Silverstein, S. C.** (1987). Tubular lysosome morphology and distribution within macrophages depend on the integrity of cytoplasmic microtubules. *Proc. Natl. Acad. Sci. USA* **84**, 1921-1925.

**Tapper, H. and Sundler, R.** (1990). Role of lysosomal and cytosolic pH in the regulation of macrophage lysosomal enzyme secretion. *Biochem. J.* **272**, 407-414.

**Tsang, A. W., Oestergaard, K., Myers, J. T. and Swanson, J. A.** (2000). Altered membrane trafficking in bone marrow-derived macrophages. *J. Leukocyte Biol.* **68**, 487-494.

**Tsien, R. Y.** (1980). New calcium indicators and buffers with high selectivity against magnesium and protons: design, synthesis, and properties of prototype structures. *Biochem* **19**, 2396-2404.

**Tsien, R. and Pozzan, T.** (1989). Measurement of cytosolic free $Ca^{2+}$ with

Quin2. In *Methods in Enzymology*, Vol. 172 (ed. S. Fleischer and B. Fleischer), pp. 230-262. New York: Academic Press.

**Vescovi, E. G., Soncini, F. C. and Groisman, E. A.** (1996). $Mg^{2+}$ as an extracellular signal: environmental regulation of Salmonella virulence. *Cell* **84**, 165-174.

**Watts, C.** (1997). Capture and processing of exogenous antigens for presentation on MHC molecules. *Annu. Rev. Immunol.* **15**, 821-850.

**Williams, R. J. P.** (1999). Calcium: The developing role of its chemistry in biological evolution. In *Calcium as a Cellular Regulator* (ed. E. Carafoli and C. Klee), pp. 3-27. New York: Oxford University Press.